JOURNAL OF MATERIALS SCIENCE 15 (1980) 1463–1468

Deformation kinetics by crazing in glassy polymers

M. KITAGAWA, Y. SAKAI
Department of Mechanical Engineering, Faculty of Technology, Kanazawa University, Kanazawa, Japan

M. KAWAGOE
Department of Mechanical Engineering, Toyama Technical College, Toyama, Japan

In order to confirm the proposed theory of the plastic deformation caused by crazing, the theoretical deformation curves derived from the dislocation analogue were calculated using the data of craze behaviour measured under static tension and compared with the experimental results of creep and constant strain-rate tension in PMMA and PVC plates wetted by kerosene as a crazing agent. Favourable agreement between the theoretical and experimental results may provide evidence that the proposed method is valuable for estimating the amount of the plastic strain caused by crazing.

1. Introduction

A large number of electron microscopic observations suggest that crazed matter consists of highly oriented polymer fibrils and small cavities. Therefore, crazes which nucleate and grow on the surface of a specimen cause a platic strain (craze strain) and then promote fracture. For instance, the yield point associated with crazing becomes much lower than the shear yield point without crazing. Since, thus, the initiation and growth of crazes play an important role in the deformation kinetics of high polymer solids, the theoretical analysis of the deformation behaviour by crazing is of considerable interest.

In the previous paper [1], by applying the Johnston–Gilman theory for dislocations [2], the deformation curves of polycarbonate (PC) thin plates wetted by kerosene were calculated for a variety of testing conditions as follows. (1) The experimental data of the growth rate and density of craze under static tension were regulated in accordance with a simple rate theory. (2) The equations, which determine the stress–strain relations of creep and constant strain-rate tension, were constructed based on the dislocation analogue and numerically solved using the regulated craze data. (3) The calculated results were compared with the experimental ones. Although some of the computed results such as high strain-rate tensile and stress–relaxation curves somewhat departed from the experimental results, the theoretical calculations could explain the experimental trends on the whole. Hence, it was concluded that the dislocation analogue is valuable for understanding the deformation kinetics by crazing.

In this paper, for the purpose of confirming the previously proposed theory, further experiments were performed using poly vinyl chloride (PVC) and poly methyl methacrylate (PMMA) plates under the action of a crazing agent, kerosene, and were compared with the calculated results.

2. Theoretical expressions

According to the dislocation analogue, the strain ϵ_c caused by crazing can be described by [3, 4]

$$\epsilon_c = \rho_v ba \qquad (1)$$

where ρ_v is the craze density which means the number of crazes per unit volume, b is the opening displacement of craze and a is the area of craze. This equation is formally identical with the relation derived from the dislocation dynamics. Since crazing is a surface phenomenon except for particle-filled polymers such as ABS and HIPS, the surface density of craze should be used in place of the volume density in Equation 1. For relatively thin

0022–2461/80/061463–06$02.60/0

specimens, Equation 1 can be rewritten as

$$\epsilon_c = \rho b\, a/z \tag{2}$$

where ρ is the number of crazes per unit surface area and z is the thickness of specimen. As described in the previous papers [1, 5], the simplifying assumptions of the shape of craze lead to

$$\epsilon_c = K\rho l^p/z \tag{3}$$

where K is the shape factor, l is the craze length measured on the specimen surface and p is the constant. If b is assumed to be constant, p is set equal to 2. When b is proportional to the length of craze, $p = 3$. In this paper, the theoretical calculations discussed below were carried out in the case of $p = 2$.

Approximate expressions of the density and growth rate of craze under static tension may be derived from a rate theory as follows [1];

$$\rho = \rho_0[1 - \exp(-mt)] \tag{4}$$

$$\rho_0 = \rho^* \exp(\alpha\sigma), \quad m = m_0 \exp(\alpha\sigma) \tag{5}$$

$$v = v_0 \exp(\beta\sigma) \tag{6}$$

where ρ_0 is the saturation density dependent on applied stress σ, ρ^* is the total number of craze nucleation sites per unit surface area, m is the rate of craze nucleation, v is the growth rate of craze and m_0, v_0, α and β are the material constants. The methods for deriving Equations 4 to 6 are reported elsewhere [1, 5, 6].

Since crazing is a surface phenomenon, the stress difference between the specimen interior where no crazes exist and the surface layer where many crazes nucleate and grow may arise when the specimen is massive. Comparison between the theoretical and experimental results for massive polymers will be reported in future. Here, we consider the deformation behaviour of a specimen which is so thin that the stress distribution is assumed to be uniform over the entire cross-section.

As shown in the previous paper [1], combining Equations 4 and 6 with Equation 3 leads to the craze strain ϵ_c at time t

$$\epsilon_c = Kz^{-1}\int_0^t m\rho_0 g\left[\int_\tau^t v\,\mathrm{d}\xi + l_0\right]^2 \mathrm{d}\tau \tag{7}$$

where l_0 is the initial length of craze, and $g = \exp(-m\tau)$ for constant stress condition or $g = 1$ for changing stress condition.

The total strain ϵ is given by the sum of the elastic strain ϵ_e and the craze strain ϵ_c

$$\epsilon = \epsilon_e + \epsilon_c. \tag{8}$$

The elastic strain is given by

$$\epsilon_e = \sigma/M \tag{9}$$

where M is the elastic modulus which exhibits nonlinear behaviour in high polymer solids. The modulus M can be obtained as a function of applied stress from the stress–strain curves without crazing. Equation 8, the equation governing the stress–strain relation associated with crazing, is a Voltera-type integral equation with respect to σ.

Equation 7 for creep and Equation 8 for constant strain–rate tension were numerically calculated with the incremental expressions with respect to time.

3. Experimental procedure

The materials used are PMMA and PVC plates 1 mm thick (Acrylite, Mitsubishi Rayon Co, and Takiron Plate, Takiron Co, Japan). The craze strain of PMMA prior to fracture is very small compared with that of PVC, and PMMA is more brittle than PVC. Hence, PMMA may be useful for understanding the mechanism of fracture caused by crazing. Dumb-bell shaped specimens (gauge section 10 x 20 mm) were cut from them, and then annealed for 1 h at 110° C for PMMA and 70° C for PVC and cooled in an oven.

The main part of a testing machine used for observing the craze behaviour under static tension is shown in Fig. 1. The jigs (J), the moving direction of which are restricted by the walls (W), are devised to run easily through the roller bearings (B) set between the walls and jigs. The tensile force transmitted from a loading system with a lever type is applied to the specimen (S) through the axis (A). The growth rate and density of craze were measured by an optical microphotographs. The experimental details of creep and constant

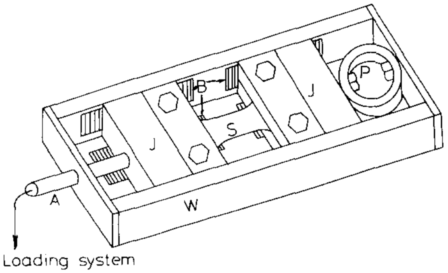

Figure 1 Illustration of the main part of the creep testing machine.

strain-rate tension are described elsewhere [1, 5]. All the tests were carried out at 20 ± 1° C under the action of a crazing agent, kerosene.

4. Discussion

The craze densities of PMMA measured under static tension are shown in Fig. 2 where the solid lines are drawn based on the theoretical Equations 4 and 5. Since the measured values were considerably scattered for each specimen, the average values were plotted. The result of PVC, which is reported elsewhere [5], is very similar to this result. The results for both polymers show good agreement between the theoretical and experimental trends. The experimental constants used for the calculations are chosen as follows;

$$\begin{aligned} \text{PMMA:}\quad \rho_0 &= 1.7\times10^{-2}\exp(1.2\sigma),\\ m &= 5.19\times10^{-6}\exp(1.2\sigma)\\ \text{PVC:}\quad \rho_0 &= 1.7\times10^{-3}\exp(2.0\sigma),\\ m &= 5.20\times10^{-7}\exp(2.0\sigma) \end{aligned} \qquad (10)$$

where the units of ρ_0, σ and m are mm^{-2}, kg mm^{-2} and sec^{-1}.

Numerous measurements of the craze length with an optical microscope show that the length varies linearly with time. The craze growth rates, the slopes of the growth curves, showed large variations even on the same specimen. The mean values are plotted as a function of applied stress in Fig. 3. The solid lines in Fig. 3 are drawn based on Equation 6 with the following constants;

$$\begin{aligned} \text{PMMA:}\quad v_0 &= 2.46\times10^{-6}\,\text{mm sec}^{-1},\\ \beta &= 1.96\,\text{mm}^2\,\text{kg}^{-1}\\ \text{PVC:}\quad v_0 &= 3.13\times10^{-8}\,\text{mm sec}^{-1},\\ \beta &= 2.57\,\text{mm kg}^{-1}. \end{aligned} \qquad (11)$$

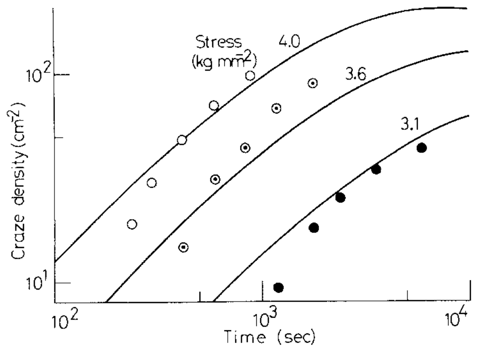

Figure 2 Comparison of theoretical (——) and experimental variations of craze densities with time at different applied stresses in PMMA.

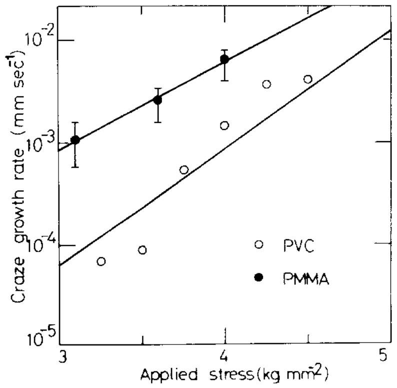

Figure 3 Effect of applied stress on the mean growth rate of craze under static tension in PMMA and PVC. The solid lines drawn empirically are used for the theoretical calculations.

The elastic modulii for both polymers were obtained from the stress–strain curves tested in air to be

$$\begin{aligned} \text{PMMA:}\quad M &= 88.4 - 2.37\sigma - 1.03\sigma^2\,\text{kg mm}^{-2}\\ \text{PVC:}\quad M &= 112.7 + 2.26\sigma - 1.32\sigma^2\,\text{kg mm}^{-1}. \end{aligned} \qquad (12)$$

Since the strain-rate dependence of M is very small, the above relations of M to σ are used for all the strain-rate ranges tested.

As stated above, all the material parameters required for the numerical calculations were derived experimentally except for the value of K. The constant K, which includes some uncertainties, was determined so that the calculated curves might fit well the experimental results. The values of K for both polymers, chosen in this way, are $K = 2.4\times10^{-3}$ mm for PMMA and $K = 1.9\times10^{-3}$ mm for PVC. The thickness b of dry or intrinsic craze is usually in the range of 0.1 to 1 μm, as reported by many workers (e.g. [7]). The recent investigation by Verheulpen-Heymans [8] has shown that the thickness in PC amounts to about 3 μm. Wet craze may be thicker than a dry one because of softening of the craze–matrix interface due to some environmental attack. If the thickness of wet craze is assumed to be 3 μm, the penetration width of craze in the direction of the interior of the specimen is obtained from the values of K, to be 0.3 to 0.4 times of the length of craze for both polymers used. This may be comparable with the experimental results of Brown *et al.*: 0.5 to 1.0 for PCTFE and 0.1 to 0.2 for PMMA [9].

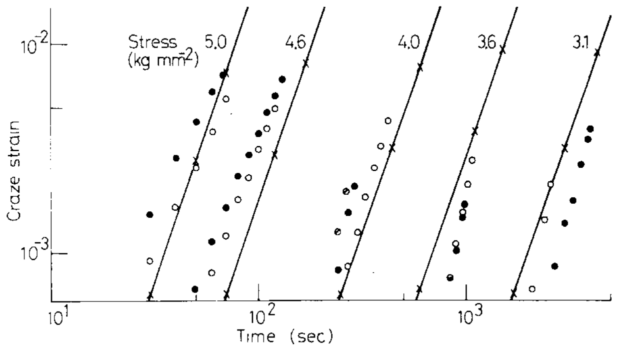

Figure 4 Comparison between theoretical (——) and experimental (○, ●) craze creep strain in PMMA. The crosses (×) denote the values calculated from Equation 13 with the constants given by Equation 14. The open and solid circles show the experimental data at the applied stresses indicated.

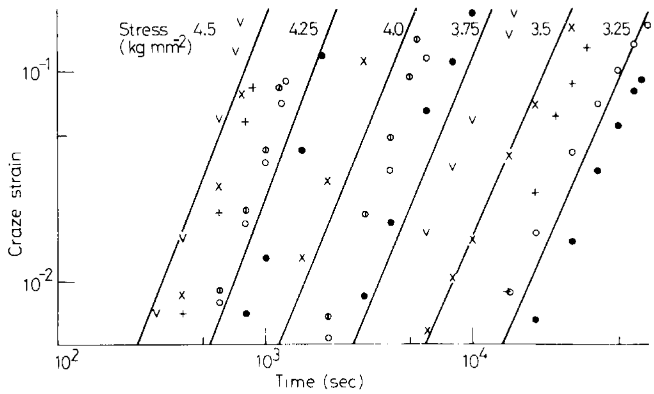

Figure 5 Comparison between theoretical (——) and experimental (●, ○, ⦶, ×, +, v) craze creep strains in PVC. ●, ○, 3.25 kg mm^{-2}; +, ×, v, 3.5 kg mm^{-2}; ●, ○, ⦶, 3.57 kg mm^{-2}; ×, 4.0 kg mm^{-2}; ●, ○, ⦶, 4.25 kg mm^{-2}; ×, +, v, 4.5 kg mm^{-2}.

First, we consider the creep deformation curves. The craze creep strain ϵ_c, the total strain minus the strain of specimen tested in air, was replotted on a log ϵ_c versus log (time) diagram in Figs. 4 and 5. Except for the fact that the craze strain of PVC is much greater than that of PMMA, the experimental trends for both polymers are very similar. The theoretical results calculated from Equation 7, which are shown by the solid lines in the figures, may explain the experimental tendencies. The theoretical computations can be numerically approximated by

$$\epsilon_c = \epsilon_{co} \exp(\eta\sigma) t^n \qquad (13)$$

where t is the time and ϵ_{co}, η and n are the material constants. The crosses in Fig. 4 denote the values calculated based on Equation 13 with the constants

$$\epsilon_{co} = 2.45 \times 10^{-21}, \quad \eta = 6.08\,\mathrm{kg}^{-1}\,\mathrm{mm}^2$$
$$n = 2.86. \qquad (14)$$

The approximate Equation 13 is found to be in good agreement with the theory over the entire ranges of applied stress. The value of n, which is independent of applied stress, is comparable with the value 3 proposed by Brown *et al.* [9]. Equation 13 is identical to the commonly used creep equation. Therefore, the theory may provide a physical foundation for this widely used equation formally derived from rate theory. However, the other equation used widely, i.e. $\epsilon_c = \epsilon_{co}\sigma^m t^n$ where ϵ_{co}, m and n are the constants, may not always be a good approximation of the present theory.

The stress–strain curves under constant strain rate tension are now discussed. The equation governing the deformation curves is obtained by combining Equations 7, 8 and 9 to give

$$\dot{\epsilon}t = \sigma/M + Kz^{-1}\int_0^t m\rho_0 \left[\int_\tau^t v\,d\xi + l_0\right]^2 d\tau \qquad (15)$$

where $\dot{\epsilon}$ is the strain rate. The numerical calculations were carried out with the experimental constants mentioned above. Comparisons between the theoretical and experimental curves at different strain rates are shown for both PMMA and PVC in Figs. 6 and 7. Although a quantitative difference between theory and experiment exists at a high strain rate of 0.2 min^{-1} in PVC, agreement between them is favourable on the whole. This discrepancy at a high strain rate may arise from the over-estimation of the craze growth rate. At a high

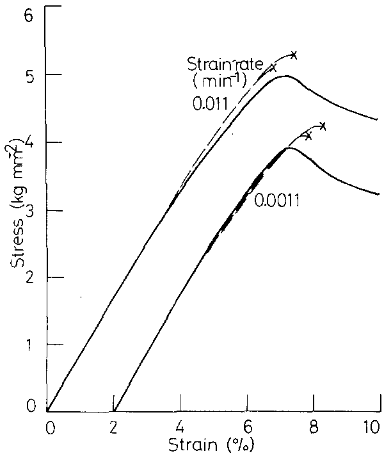

Figure 6 Comparison between theoretical (——) and experimental (– – –) stress–strain curves in PMMA. The crosses denote fracture points.

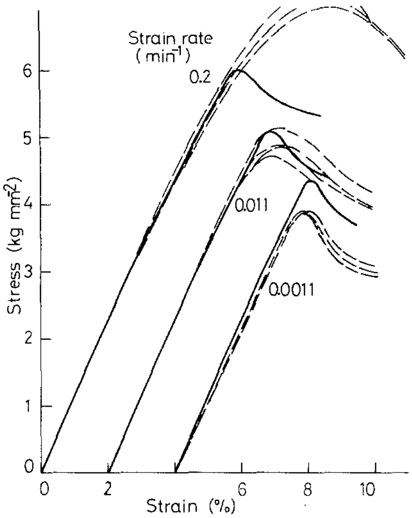

Figure 7 Comparison between theoretical (——) and experimental (– – –) stress–strain curves in PVC.

strain rate, the craze growth rate in the high stress range is expected to be much lower than the values given by Equation 6 since the high density of crazes causes mutual interaction between individual crazes and the growth of craze is arrested by the plastic or shear bands developed in front of the craze as shown in Fig. 8. The observation by a polarizing microscope showed that the shear band formation occurs at a relatively high stress level, but not at a low stress range.

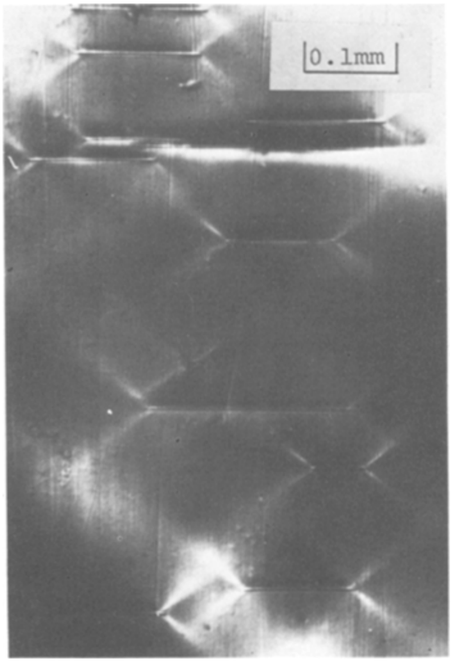

Figure 8 Shear bands at craze tip observed by an polarizing microscope.

The theory may explain the yield drop behaviour of PVC which becomes gentle with increasing strain-rate, whereas the experimental yield drop behaviour of PMMA is unknown because fracture occurs just before or after craze yielding.

5. Conclusions

In order to confirm the previously proposed theory derived from the dislocation analogue, further experiments were performed in the presence of a crazing agent using thin plates of PMMA and PVC and compared with the theoretical results. Good agreement between theory and experimental results indicates that the theory is valuable for estimating the craze plastic deformation, as predicted in the previous paper. However, the theory may not be applied to the deformation curves in the high stress range where shear bands initiate in front of craze and, yielding then occurs with a mixed mode of shearing and crazing.

According to the present theory, the specimen-size effect on the plastic deformation is described only by the term of specimen thickness, since crazes are assumed to be distributed uniformly over the cross-section of the specimen. However, this assumption may not be valid for massive polymers. Since the stress difference between the crazed surface layer where crazes nucleate and grow and the interior with no crazes may exist for a thick specimen, this difference should be taken into account in the theory. Thus, the size effect derived from the theory including this discrepancy may be expected to be greater than that from the present theory. Further investigations will be required.

References

1. M. KITAGAWA and M. KAWAGOE, *J. Mater. Sci.* **14** (1979) 953.
2. W. G. JOHNSTON and J. J. GILMAN, *J. Appl. Phys.* **30** (1959) 129.
3. J. HOARE and D. HULL, *Phil. Mag.* **26** (1972) 443.
4. N. BROWN, *J. Polymer Sci. A-2* **11** (1973) 2099.
5. M. KITAGAWA and M. KAWAGOE, *ibid A-2* **17** (1979) 663.
6. *Idem, J. Soc. Mater. Sci. Japan* **27** (1978) 995.
7. R. P. KAMBOUR, *J. Polymer Sci. Macromol. Rev.* **7** (1973) 1.
8. N. VERHEULPEN-HEYMANS, *polymer* **20** (1979) 356.
9. N. BROWN, B. METZGER and Y. IMAI, *J. Polymer Sci. A-2* 8 (1978) 1085.

Received 29 August and accepted 30 October 1979.